



HAL
open science

Heating of proton conics by resonant absorption in a multicomponent plasma: 1. Experimental evidence

Jean-Louis Rauch, François Lefeuvre, Dominique Le Quéau, Alain Roux,
Jean-Michel Bosqued, Jean-Jacques Berthelier

► To cite this version:

Jean-Louis Rauch, François Lefeuvre, Dominique Le Quéau, Alain Roux, Jean-Michel Bosqued, et al.. Heating of proton conics by resonant absorption in a multicomponent plasma: 1. Experimental evidence. *Journal of Geophysical Research Space Physics*, 1993, 98 (A8), pp.13347-13361. 10.1029/92JA02255 . insu-02612308

HAL Id: insu-02612308

<https://insu.hal.science/insu-02612308>

Submitted on 19 May 2020

HAL is a multi-disciplinary open access archive for the deposit and dissemination of scientific research documents, whether they are published or not. The documents may come from teaching and research institutions in France or abroad, or from public or private research centers.

L'archive ouverte pluridisciplinaire **HAL**, est destinée au dépôt et à la diffusion de documents scientifiques de niveau recherche, publiés ou non, émanant des établissements d'enseignement et de recherche français ou étrangers, des laboratoires publics ou privés.

Heating of Proton Conics by Resonant Absorption in a Multicomponent Plasma

1. Experimental Evidence

JEAN LOUIS RAUCH,¹ FRANÇOIS LEFEUVRE,¹ DOMINIQUE LE QUÉAU,² ALAIN ROUX,³

JEAN MICHEL BOSQUED,⁴ AND JEAN JACQUES BERTHELIER,⁵

ELF emissions observed on the low-altitude AUREOL 3 satellite are seen in association with H⁺ ions at large pitch angle. The flux in the upward direction for ~120° pitch angle is found to be equal to or larger than the flux at ~60° pitch angle, which provides evidence for transverse acceleration at or below the spacecraft. These emissions have a sharp lower-frequency cutoff of the transverse components of the electric field and a narrow peak at, or, more precisely, just below the proton gyrofrequency f_{H^+} . This narrow peak is more easily seen on the parallel component and appears as a narrow line on the spectrogram of this component. A statistical study of the occurrence of this line at $f \sim f_{H^+}$ is presented. It is shown that this line is observed at relatively high invariant latitude within the light ion trough where a strong depletion of thermal H⁺ ions occurs. Detailed analysis of ELF waves observed just below f_{H^+} demonstrates that they propagate in the left-hand mode. These observations are interpreted as a signature of mode conversion from a fast magnetosonic mode into a slow proton cyclotron mode. It is suggested that this slow proton cyclotron wave can accelerate protons up to a few hundreds electron volts in the transverse direction. This mode conversion process can operate over a much broader of large altitude range than covered by AUREOL 3; it is a likely candidate for explaining the formation of H⁺ conics. Theoretical calculations that support the above conclusions are given in a companion paper by Le Quéau et al. (this issue).

1. INTRODUCTION

Ion conics result from the combination of a transverse acceleration, followed by an upward motion driven by the magnetic mirror force. Ion conics therefore play a key role in the population of the magnetosphere with ions extracted from the ionosphere. Many papers have given experimental evidence [Ungstrup et al., 1979; Klumpar, 1979; Yau et al., 1984, 1985a,b; Klumpar, 1986 and references therein] and theoretical explanations [Lysak et al., 1980; Okuda and Ashour-Abdalla 1981, 1983; Ashour-Abdalla and Okuda, 1984; Chang et al. 1986; André et al. 1990 and references therein] for the formation of the conical pitch angle distribution of ions. The narrowness of observed angular distributions suggests that a heating mechanism should be able to accelerate ions in a relatively narrow angular range around 90°. Several mechanisms have been proposed in the literature to heat the H⁺, He⁺, and O⁺ ions in the perpendicular direction. Various scenarios have been proposed. Ungstrup et al. [1979], Okuda and Ashour-Abdalla [1981], and many others have suggested that electrostatic ion cyclotron waves (EICWs), driven unstable by a field-aligned current, heat the ions in the transverse direction. The main difficulty with this mechanism is that electrons diffuse rapidly in velocity space, in the V// direction, thus leading to a plateau.

Hence the instability is rapidly quenched unless flowing electrons are continuously fed into the system, as illustrated by numerical simulations by Okuda and Ashour-Abdalla [1983]. Furthermore, the relationship between EICWs and conics is not found to be a common feature. The existence of one of the two modes, electrostatic O⁺ cyclotron waves or electrostatic lower hybrid waves, is possible with the presence of ion conics. But no evidence is found for the existence of H⁺ cyclotron waves during the perpendicular ion acceleration [Kintner and Gorney, 1984]. Retterer et al. [1986] and Chang and Coppi [1981] have suggested that lower hybrid waves could heat ionospheric ions in the transverse direction. The same remark as above, applied to the correlation between lower hybrid resonance noise and conics, is not overwhelming; other mechanisms must be considered to heat ions. Lemnartsson [1983] and Sharp et al. [1983] have suggested a different mechanism, where a potential drop applied in a direction transverse to B₀ accelerates ions. Recently, Lundin et al. [1990] expanded this idea and suggested that the transverse electric field of ultralow-frequency Alfvénic fluctuations could accelerate the ions. They do not assume any resonance between the Alfvén waves and the ions; their mechanism relies on the perpendicular velocity increment associated with random increases of the electric field of the Alfvén waves, which are indeed simultaneously observed. Lundin et al. [1990] were able to demonstrate a good correlation between the level of the Alfvén waves and the transverse acceleration/heating which provides a strong argument in support of the mechanism they propose. It is obvious, however, that a nonresonant process is a priori much less efficient than a resonant one.

Crew et al. [1990] also suggested that Alfvén waves accelerate/heat the ions. In their mechanism, they assume that an Alfvén wave propagates, its frequency matches the local ion gyrofrequency somewhere. They also assumed that when this occurs, the Alfvén wave still has a finite left-hand component that is sufficient to accelerate/heat the ions. More recently, Johnson et al. [1989] suggested that resonant absorption can account for the heating of ions.

The present paper aims at investigating a process responsible for the transverse ion acceleration: the first stage in the formation of conics. We further investigate the relation between Alfvén waves

¹Laboratoire de Physique et Chimie de l'Environnement, Centre National de la Recherche Scientifique, Orléans, France.

²Entité Centre de la Recherche Scientifique du Centre de Recherche en Physique de l'Environnement, Vélizy, France.

³Centre de Recherche en Physique de l'Environnement, Centre National d'Etude des Télécommunications, Centre National de la Recherche Scientifique, Issy-les-Moulineaux, France.

⁴Centre d'Etude Spatial des Rayonnements, Centre National de la Recherche Scientifique, Toulouse, France.

⁵Centre de Recherche en Physique de l'Environnement, Centre National d'Etude des Télécommunications, Centre National de la Recherche Scientifique, Saint Maur des Fossés, France.

and the formation of ion conics, where the role of mode conversion between the magnetosonic and ion-cyclotron mode is determinant. In particular, we take advantage of waveform data collected on the five electromagnetic components by AUREOL 3 (two electric, three magnetic) to perform a detailed analysis with a high-frequency resolution at and just below the proton gyrofrequency. Furthermore, evidence for mode conversion from the fast Alfvénic mode into the slow proton cyclotron mode is given.

The paper is organized as follows: Section 2 presents a description of the instruments. Wave observations are presented in section 3 with particular emphasis on the existence of an intense line at or just below f_{H^+} . Section 4 is devoted to a statistical study of the localization of this emission in magnetic local time and invariant latitude, and comparisons are made with the position of the light ion trough (LIT). In section 5 we investigate the relationship between waves and ion conics. A detailed study of wave characteristics is given in section 6, where the propagation mode is identified.

2. INSTRUMENTATION

AUREOL 3 was a three-axis-stabilized satellite launched on September 21, 1981, into a quasi-polar orbit (apogee 2012 km, perigee 408 km, inclination 82.5°, period 109.5 min). Results presented here are based on data from three experiments: TBF-Onch, Dyction, and Spectro, from ARCAD 3.

The TBF-Onch experiment [Berthelier et al., 1982b] performed measurements of the wave field components in the ELF/VLF frequency range from 10 Hz up to 16 kHz, and several modes of operation are possible. In the mode considered here, two electric and three magnetic field components were simultaneously measured in the 10-1500 Hz band, and waveforms were transmitted to the ground. One electric component, E_z , was measured by means of two spherical probes, located at the end of an insulated boom parallel to the vertical Z axis of the spacecraft. The distance between the two spheres was 2.36 m. The Z axis was approximately along the vertical, which gave an angle between 0° and 20° with respect to the local magnetic field B_0 . The second electric component, E_H , was measured by means of two spheres located on two different booms. The distance between these spheres was 7.87 m. The theory and practice of DC and AC electric field measurements in the ionosphere, using this double-probe technique, are well documented by Moser [1973]. The H direction was 11.5° off the plane perpendicular to the Z axis. As far as the magnetic components are concerned, B_z is taken along Z, whereas B_x was directed along the average velocity vector of the satellite and in a plane perpendicular to B_z , which contains also the B_{x45} component, at 45° from B_x .

The Dyction experiment [Berthelier et al., 1982a] was an ion mass spectrometer, designed for measuring the density, bulk velocity, and temperature of the thermal ionospheric ions. The counting rates of the various ions (mainly H⁺, He⁺, and O⁺), corrected for a transmission factor, allow a comparison between the various ion densities. The relative concentrations obtained are consistent with measurements performed on DE 1 and 2 [Horwitz et al., 1990]. Here, the data are mainly used to determine the location of the light ion trough [Taylor and Walsh, 1972].

The Spectro experiment [Bosqued et al., 1982] was designed to measure the energy spectra, and the angular distributions of ions and electrons in the energy range 0.01-21 keV/Q. In order to identify the presence of conics, we consider the results provided by the two suprathermal ion spectrometers which measured the abundance of ionospheric (H⁺, He⁺, O⁺, O⁺⁺) and magnetospheric (H⁺, He⁺⁺) ions, from several electron volts to 14 keV/Q, and in

two fixed directions, 60° and 120° with respect to the vertical axis of the satellite, that is, essentially along the magnetic field. The pitch angles analyzed by these two spectrometers were thus practically constant during a crossing of the auroral region (60°-70° and 120°-130°, respectively, for the northern hemisphere). Thus, when the flux of H⁺ ion is enhanced and larger at ~120° than at 60°, we can expect that a transverse acceleration has occurred somewhere below or near the spacecraft. This is how "conics" are defined in the rest of the paper. However, it is clear that the present measurements cannot unambiguously identify conics, nor is it certain that no conics were missed at pitch angles not covered by the experiment. Still, when an event fulfilling the above criteria was recorded, a transverse acceleration of the corresponding ion species certainly took place below the spacecraft.

The data referred to in this study have been recorded over limited time intervals, when the satellite was passing over one of the high-latitude receiving telemetry stations. Even considering one year of data, a uniform coverage in the MLT domain cannot be achieved.

3. WAVE OBSERVATIONS

Waves observed around the local proton gyrofrequency at medium and high invariant latitudes show similar features, regardless of altitude and local time. As an illustration, two typical orbits have been chosen. They both show ELF wave observations performed in the dayside MLT sector and the northern hemisphere. The two examples presented here are taken at two different altitudes. Plate 1 and Figure 2 show data collected at a relatively low altitude (~1000 km) during orbit 4349. Plate 2 shows data from orbit 3162, corresponding to observations at higher altitude near the apogee, at about 2000 km. For each orbit, the time frequency characteristics of the waves will be discussed. For orbit 3162, the spectral characteristics in the vicinity of the local proton gyrofrequency (f_{H^+}) will be examined in detail, and the associations with particle data will be shown.

Orbit 4349

Plate 1 presents simultaneous electron and ELF wave spectrograms recorded at a relatively low altitude (~1000 km) near the polar cusp. From top to bottom, plate 1a shows the flux of downgoing electrons (color coded) over 200 eV to 20 keV; plates 1b to 1e show dynamic spectra of magnetic and electric components perpendicular (B_x, E_H) and parallel (B_z, E_z) to the local magnetic field B_0 , over a frequency range from 10 to 1200 Hz. AUREOL 3 was moving from the northern polar cap toward the auroral zone in the dayside sector (13-14 MLT). The polar cusp, and adjacent regions as defined by the precipitation of low-energy ($E \leq 500$ eV) electrons, were crossed around 13 MLT from 0912:30 UT ($\Lambda \sim 83^\circ$) to 0915:30 UT ($\Lambda \sim 74^\circ$). During the period 0915-0922 UT, an intense hiss event was recorded on all field components, with a bandwidth varying from 200 to 700 Hz. This event can be divided into two time periods.

During the first period, from 0915:00 to 0919:30 UT, corresponding to an invariant magnetic latitude $63^\circ \leq \Lambda \leq 70^\circ$, the frequency bandwidth was broader and extended below the local proton gyrofrequency, $f_{H^+} = 550$ Hz. This was observed in association with enhanced energetic electron fluxes (~3 KeV). Similar associations have been reported by several authors [Gurnett and Frank, 1972ab; Mosier and Gurnett, 1972; Laaspere and Hoffman, 1976; Gorney et al., 1982], who concluded that the observed broadband ELF hiss emission was generated by downgoing electrons. Simultaneously, a strong enhancement was observed in the E_z component, at or close to the local proton gyrofrequency, as will be further discussed.

ORB 4349 17/08/1982 TROMSOE AUREOL-3

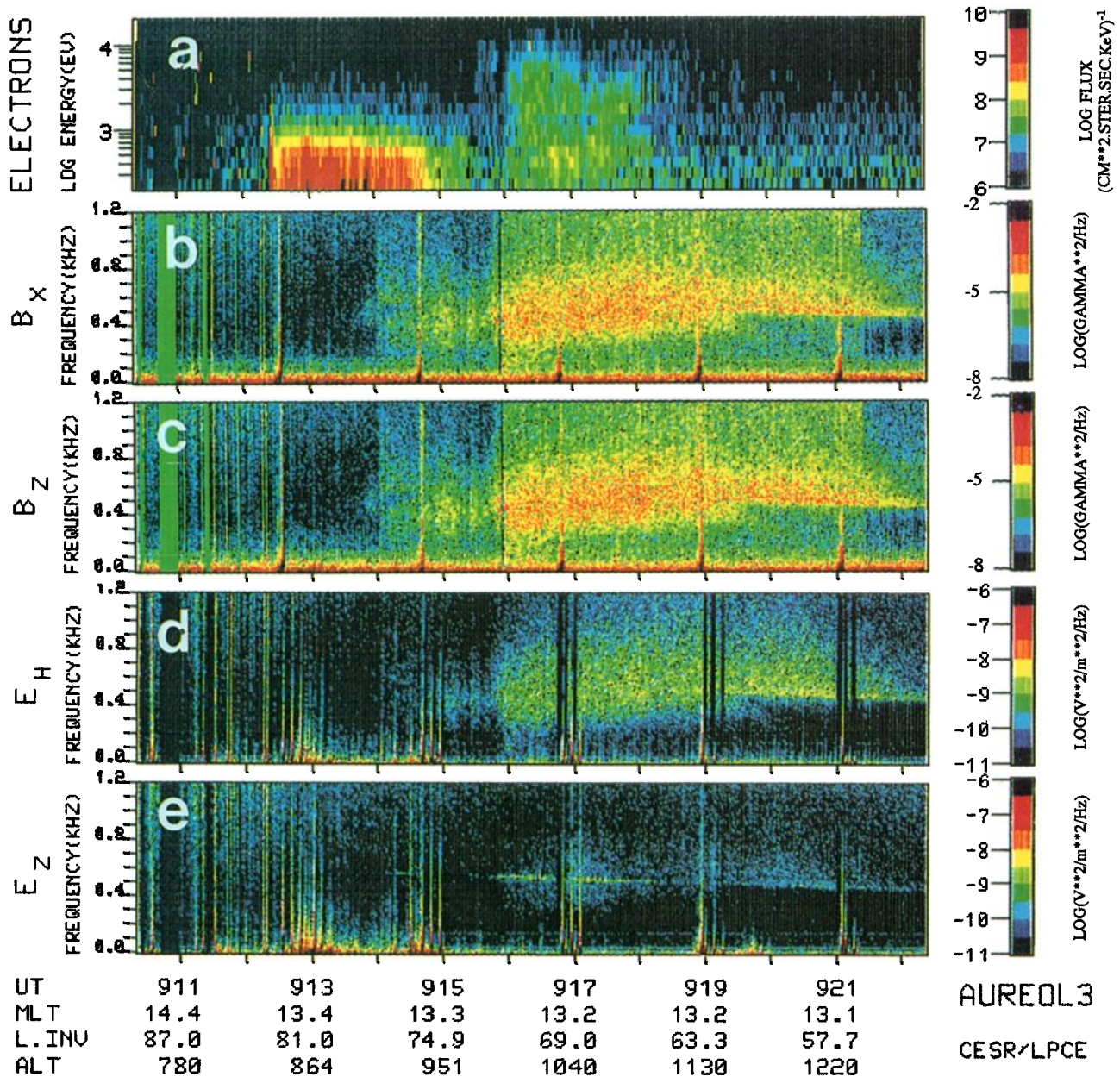


Plate 1. Spectrogram of the parallel (E_z , B_z) and perpendicular (E_h , B_x) electric and magnetic components and electron precipitation (200 eV to 4 KeV) taken on August 17, 1982. ELF hiss emission is associated with the electron precipitation. ELF hiss exhibits a sharp cutoff at the vicinity of the proton gyrofrequency f_{H^+} . A strong line of a few hertz width is detected just below the frequency f_{H^+} in the electric component E_z during the time period 0914:00-0921:00 UT.

In the second period, from 0919:30 to 0922:00 UT, at $\Lambda \leq 63^\circ$, the hiss presents a sharp lower-frequency cutoff at f_{H^+} . Although not clearly shown by this figure, the wave power was weaker than during the first period. The intensity of the f_{H^+} line observed on the E_z component is still present but weaker. Moreover, the electron precipitation has disappeared. The sharp lower-frequency cutoff observed during the latter period is well documented in the literature. Sharp frequency cutoff close to the H⁺ gyrofrequency have been observed at low altitudes by *Gurnett and Burns* [1968] as well as in the equatorial region by *Rauch and Roux* [1982], at f_{H^+} . As shown by *Gurnett and Burns* [1968], a cutoff close to f_{H^+} was observed whenever the following two conditions were fulfilled:

- (1) The H⁺ density is much smaller than that of heavier ions (e.g., O⁺, He⁺).
- (2) The angle between the wave number K and B_0 is not too small (here $\sim 50^\circ$).

The waves propagate in the nonducted magnetosonic mode. The observation of large wave propagation angles, the decreasing of the wave energy, and the absence of precipitating electrons after 0919:30 UT suggest that the sources are not on the same magnetic field lines (after 0919:30).

A detailed analysis of the line observed close to f_{H^+} during the period extending from 0915:00 to 0919:50 is presented in Figure 1. All along the pass, systematic spectral analyses were carried out with a frequency resolution of 1 Hz. For each spectrum, a search

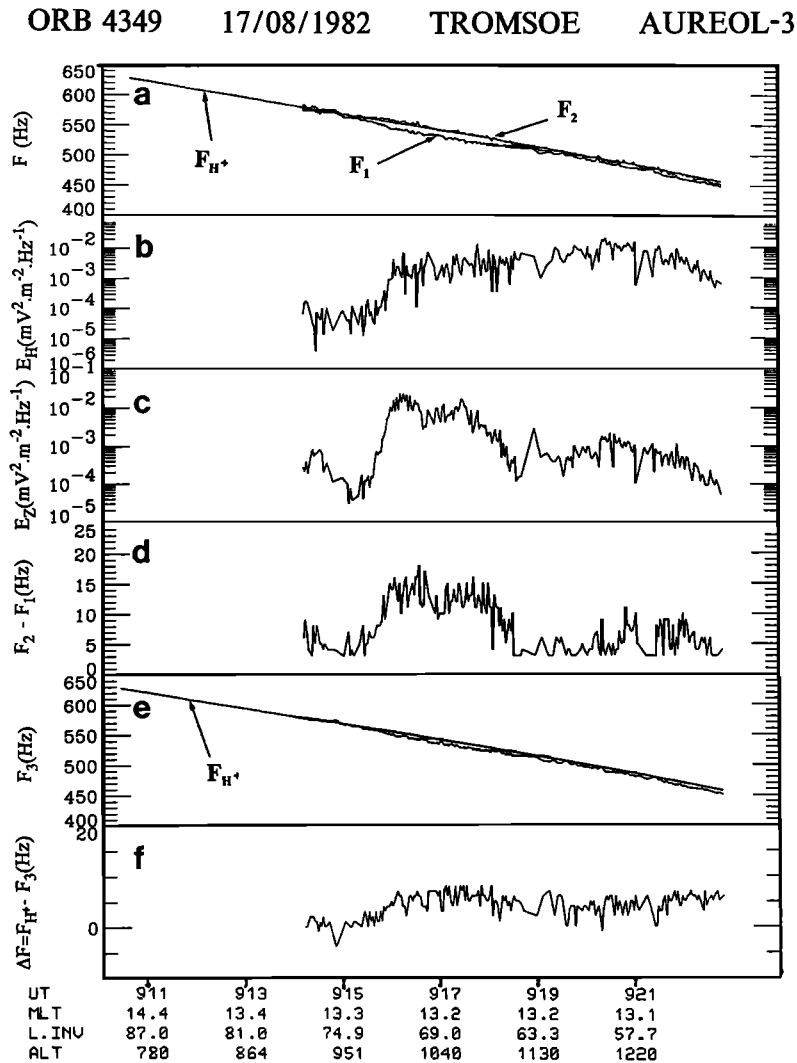


Fig. 1. Characteristics of the line seen on E_z on August 17, 1982. (a) Frequency position of the line; note that the frequency of the line follows the local proton gyrofrequency. (b) Average power of the perpendicular component (E_H). (c) Average power of the parallel component (E_Z) computed inside the line. (d) Width of the line; the maximum is around 10 Hz. (e) Frequency position of the power maximum in relation to the proton gyrofrequency, which is always below the local proton gyrofrequency. (f) Gap between the frequency of the maximum power of the line and the proton gyrofrequency, which is always around 5 Hz below the f_{H^+} frequency even when the power is weak.

for a peak in the E_z electric component was made. For each detected peak the frequencies f_1 and f_2 , corresponding to $1/e$ times the amplitude at the peak, are plotted in Figure 1a (top). The existence of a small difference $f_2 - f_1$ provides further evidence for a well-defined peak in the E_z component between 0915:00 and 0919:00 UT. From top to bottom we have plotted, versus time, the power of the peak for the perpendicular E_H (Figure 1b) and parallel E_Z (Figure 1c) components, the frequency width of the peak in the E_Z component (Figure 1d), the frequency f_3 where the power spectral density of E_Z component is maximum (Figure 1e) and finally the frequency difference $\Delta f = f_{H^+} - f_3$ (Figure 1f). The following features are worth pointing out.

1. In spite of the large frequency variation of f_{H^+} (150 Hz) over the 12 min considered, the variation of the frequency of the peak follows that of the proton gyrofrequency. Then the observed line close to f_{H^+} cannot be due to interference generated by the spacecraft.

2. The observed line close to f_{H^+} is enhanced by 2 orders of magnitude during the energetic electron precipitation.

3. The width of the emission line is about 10 Hz (Figure 1d).

4. The frequency where the electric power is maximum is always below f_{H^+} , and $\Delta f = f_{H^+} - f_{max}$ is about 5 Hz (Figure 1e) and always positive.

Orbit 3162

Plate 2 and Figure 2 are similar to Plate 1 and Figure 1, but show observations made at a higher altitude near the apogee of AUREOL 3 (2000 km) during pass 3162 over the northern hemisphere. Unfortunately, electron data are not available for this pass. Again, the spectrograms can be divided into two periods. First, before 1108 UT (below 56° magnetic latitude) the hiss is less intense and narrow-banded, and a very sharp lower-frequency cutoff is observed. One also notices an attenuation band at 450 Hz, as already pointed out by Rauch *et al.* [1985]. This latter observation will not be discussed here.

Second, after 1108:00 UT (for $\Lambda \geq 56^\circ$) the hiss is wide-banded and extends below f_{H^+} . A line at f_{H^+} shows up on the E_z spectrogram. This line is also seen on the magnetic spectrograms, particularly on the B_{X45} , but with a much weaker contrast. An increase in the magnetic energy density in the vicinity of the

ORB 3162 19/05/1982 TROMSOE AUREOL-3

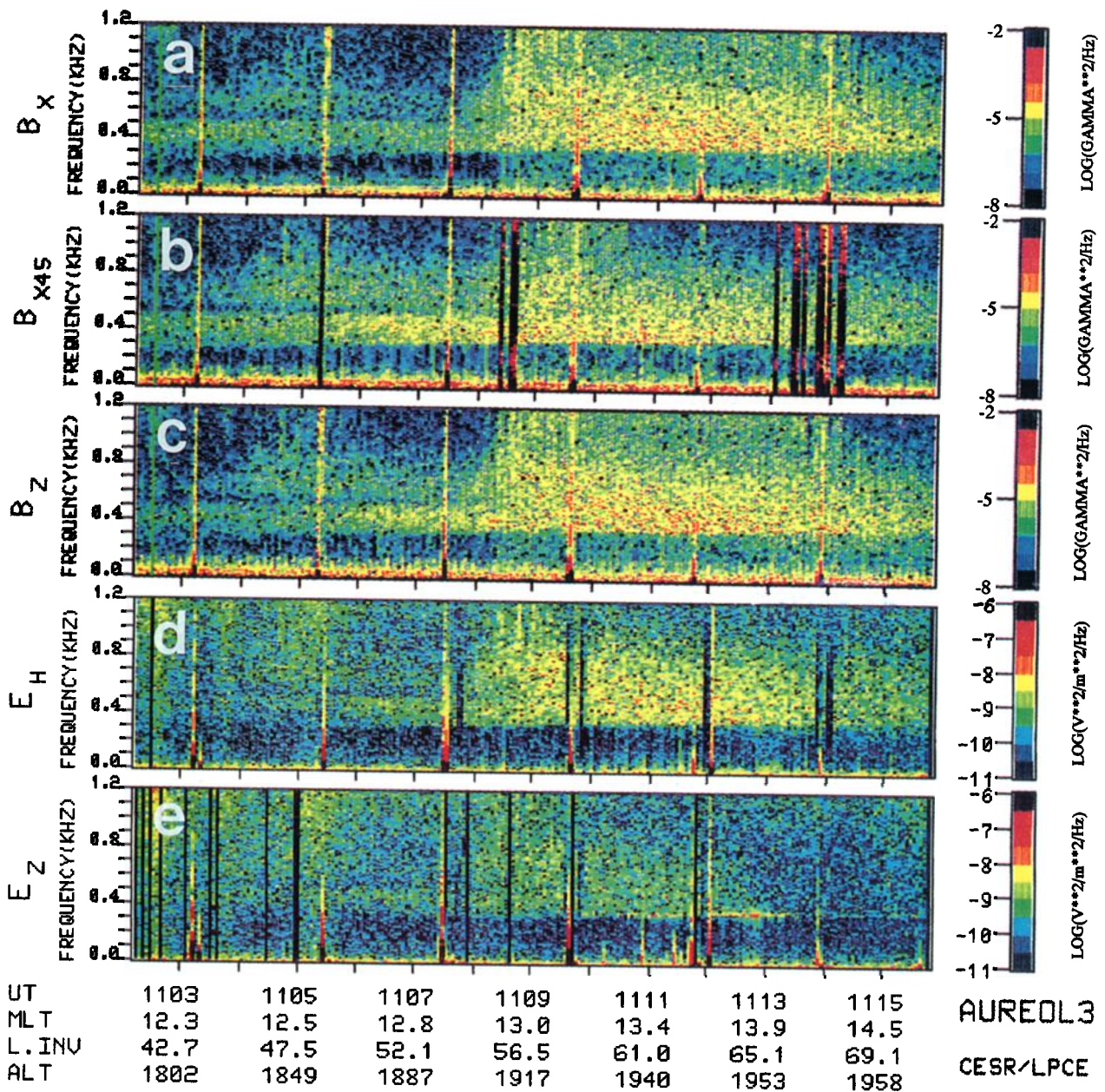


Plate 2. Same as Plate 1, but the altitude is 1000 km above.

proton gyrofrequency could be explained by a propagation effect: it could result solely from a low group velocity, close to a reflection point, thus leading to an enhanced wave energy. This explanation is not consistent, however, with the observed enhanced line on the E_z component which is a new phenomenon. Clearly, the enhanced line seen mainly on E_z has a finite bandwidth, ~10 Hz, and is significantly below f_{H+}. Figure 2 is in a format similar to Figure 1; it shows the detailed behavior of the wave energy at f ~ f_{H+}. Although f_{H+} it varies less than during pass 4349, advantage will be taken of this relatively weak variation to integrate the spectra over ~10 s, thus improving the frequency resolution. This will be explained in section 6.

4. STATISTICAL ANALYSIS

Numerous events, recorded on the TBF and Dycion experiments of the AUREOL 3 satellite above the northern hemisphere, in the

dayside MLT sector, present characteristics similar to the two cases discussed above. At high invariant latitudes, wide-band hiss is clearly associated with precipitating energetic (1-20 keV) electrons. Typically, such hiss has magnetic power spectral densities of the order of 10⁻¹ to 10⁻³ mW²/Hz, a smooth lower-frequency cutoff (decrease of the power spectral density over a 100-Hz band as seen in Plate 1, from 0915:00 to 0919:30 UT), and often an enhanced line on the E_z electric component. According to the orientation of the satellite, the E_H component may contain a weak part of the electric component parallel to B₀. In a few cases and for very specific configurations, an increase in the spectral power density in E_H is detectable in the vicinity of f_{H+}. But the line at f_{H+} is still present in E_z. Narrow-band hiss, observed at medium invariant latitude, has electromagnetic energy densities that are about 10 times lower, a sharp lower-frequency cutoff (decrease of the power spectral density over a 10-Hz band, as in Plate 1, from 0919:30 to

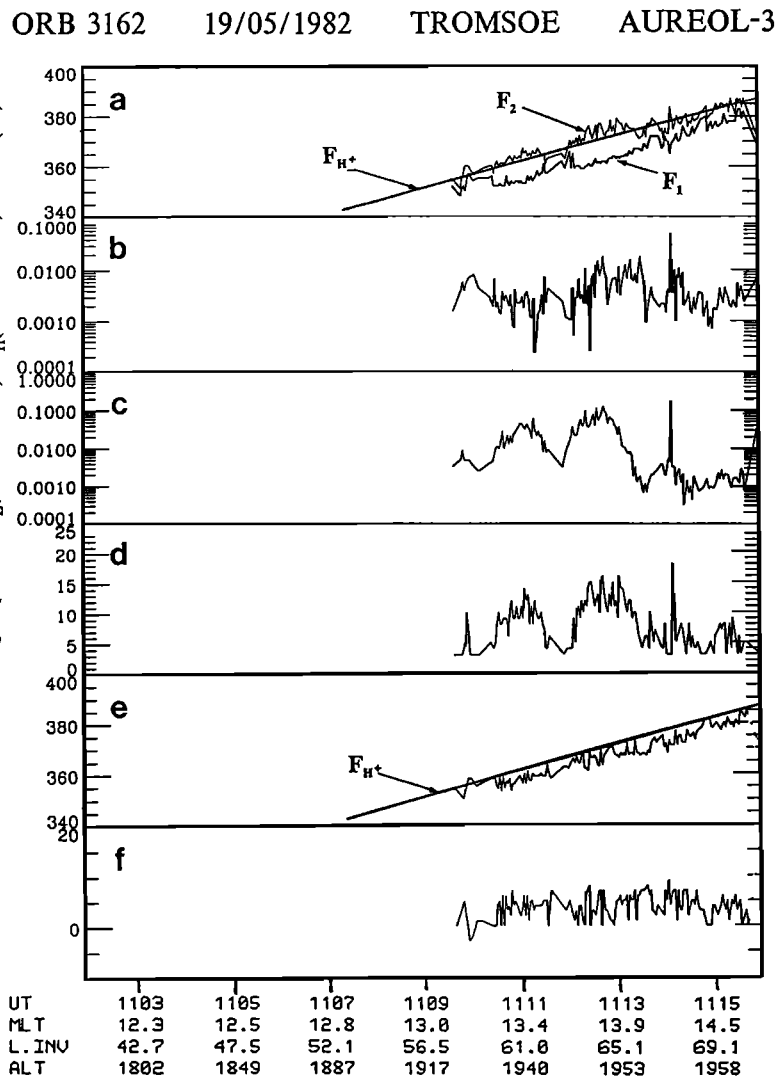


Fig. 2. Same as Figure 1, but the altitude is 1000 km above.

0922:00 UT), and generally no enhanced line on E_z . These characteristics are not associated with a detectable precipitation of energetic electrons. The situation appears more complex in the nightside sector where the magnetic and electric energy densities are usually smaller [Parrot, 1990].

Examination of the ion composition is a key issue for the understanding of the origin of this enhanced line at f_{H^+} . Direct measurements from the Dyction experiment, and indirect measurements from the ratio of the local lower-frequency cutoff to the local proton gyrofrequency [Gurnett *et al.*, 1965], show that the O⁺ ionospheric ions are dominant on the dayside for the high invariant latitude regions covered by AUREOL 3 (90 to 99%, according to the altitude of observation) whereas they can fall below 50% in the medium invariant latitude region. The boundary between these two regions corresponds to the light ion trough (LIT) defined, by Taylor and Walsh [1972]. It is defined as a depletion in the H⁺ content and possibly the He⁺ concentration [Guegan *et al.*, 1982].

In order to establish the relationship between the ion composition profiles and the presence of an enhanced line at f_{H^+} , these data were subjected to statistical analyses. One year of AUREOL 3 data has been used (October, 1 1981, to September, 30 1982). The data base is restricted to the orbits corresponding to low and moderate

magnetic activity ($K_p \leq 3+$). Moreover, records with a poor signal-to-noise ratio have been rejected. As a result, 112 distinct time intervals have been selected. When possible, i.e., when the mass spectrometer is not contaminated by radiation belt particles, the equatorward boundary of the LIT is defined as the middle value of the gradient in the H⁺ counting rate. Such an approximation is valid as long as the O⁺ counting rate does not vary too much, which is generally the case. Results are shown in Figure 3 and 4.

Figure 3 shows the occurrences of an enhanced line at f_{H^+} , as a function of MLT and invariant latitude, where each bin corresponds to 1° invariant latitude. The plots have been split into eight time intervals of 3 hours each. The upper curve represents the number of hiss events. The lower curve gives the number of observations of f_{H^+} lines observed during the same time intervals. The crosses indicate regions in invariant latitude where the LIT equatorward boundary has been determined. The asterisk gives the median position of these boundaries. Running from MLT sectors 00-03 to 21-24 we have, respectively, 9, 5, 1, 4, 13, 4, 4, and 16 LIT boundary determinations.

Clearly, the f_{H^+} lines are more common on the dayside (from 09 to 21 MLT) and at high invariant latitude (from 55° to 75°). In the 12 to 15 MLT sector, the percentage of observations of f_{H^+} lines reaches 74% at ~70°. Noting that the selected data contain several

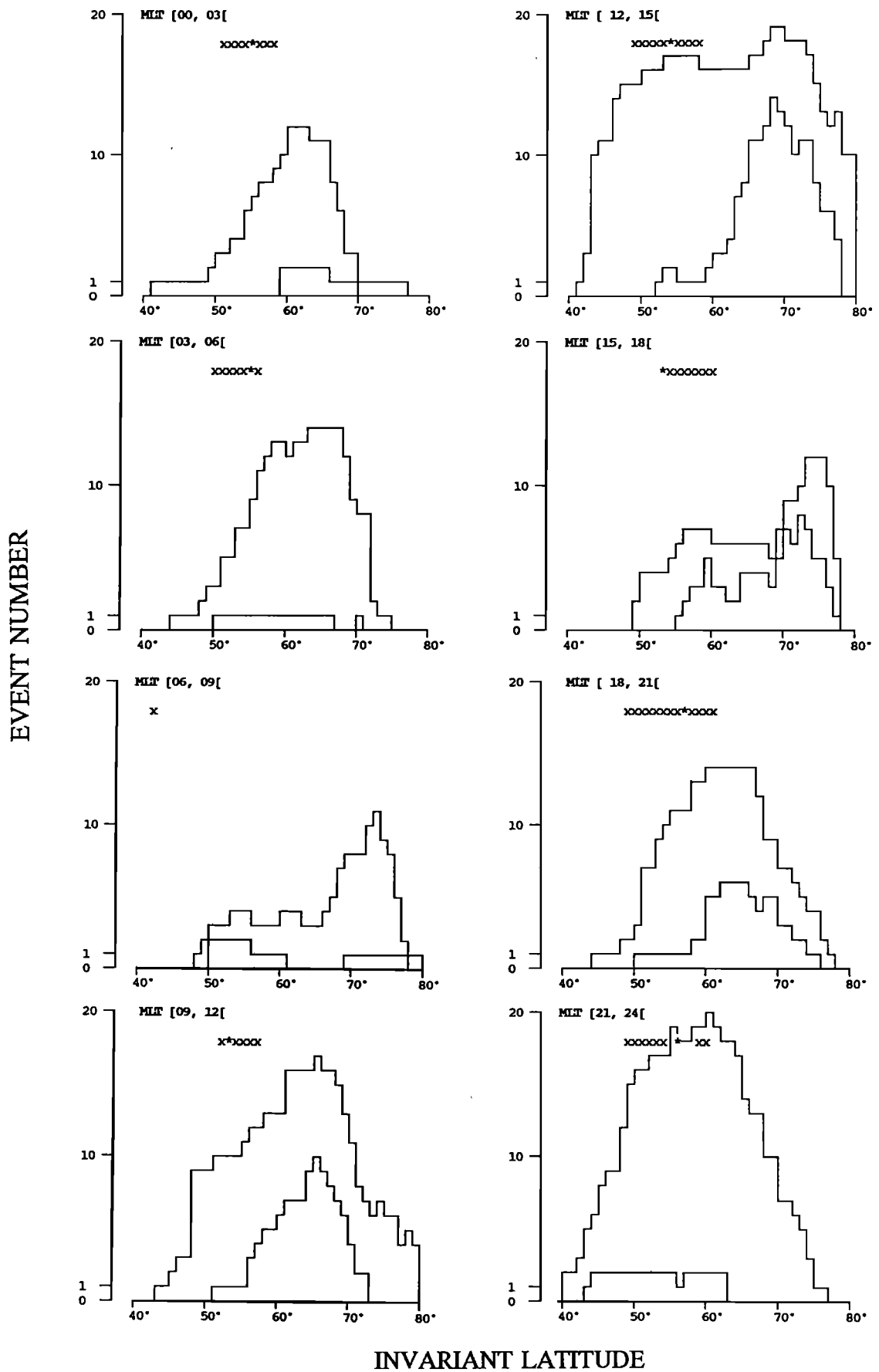


Fig. 3. Histograms showing the distribution in invariant latitude of all the hiss events (upper curve) and of the lines at f_{H+} (lower curve) observed on AUREOL 3 in 1982, during geomagnetic quiet periods. Eight MLT time intervals are considered. The crosses indicate the domain on which the LIT is identified. The asterisk represents the median value. Note that, the F_{H+} line is always inside the LIT.

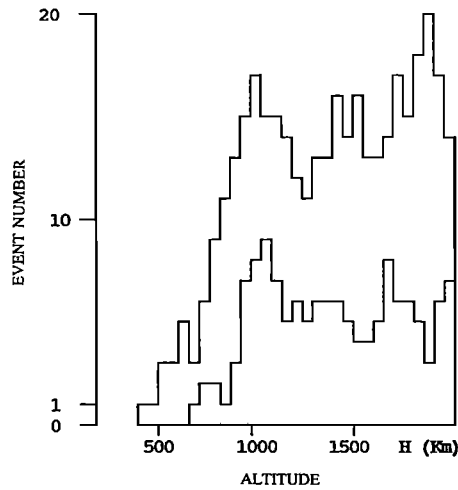


Fig. 4. Histogram showing the distribution in altitude of the hiss events (upper curve) and of the line at f_{H+} (lower curve) observed between 09 and 21 MLT in 1982, during geomagnetic quiet periods.

types of electromagnetic emissions (particularly emissions below f_{H+}), one can consider that, around noon, hiss events above f_{H+} are practically always accompanied by a f_{H+} emission line. Comparisons with the world maps of the AUREOL 3 emissions in the ELF frequency range [Parrot, 1990] show that the f_{H+} lines appear at invariant latitudes and MLT regions where the electromagnetic energy density of the hiss is maximum.

From the results presented in Figure 3, one can consider that f_{H+} lines are observed at invariant latitudes ($>55^\circ$) corresponding to the LIT regions where O⁺ ions are the dominant species. This is consistent with the positions of the equatorward boundaries of the LIT shown in Figure 3. In the 12-15 MLT sector, however, the latitude of the LIT boundaries is $\sim 15^\circ$ lower than the latitude of the f_{H+} lines. The cases where a LIT boundary and a line at f_{H+} were detected on the same orbit are enumerated in Table 1. The LIT boundary is always observed at an invariant latitude lower than that of the f_{H+} line. The only exception in the table corresponds to a difference of -1° , which is not significant.

Statistics on the altitudes of observation are given in Figure 4. The upper curve represents the observations of hiss events from 09 to 21 MLT. The lower curve indicates the occurrence of enhanced lines at f_{H+} . Relative fluctuations between the two curves are not significant; no systematic variation with altitude is found, at least below 2000 km, the apogee of AUREOL 3.

The distribution of the f_{H+} lines is in good agreement with that of conics, the latter being inferred from S3-3 data [Gorney *et al.*, 1981]. During quiet times the distribution of ion conics is uniform above 2000 km, which implies that the generation region is at a lower altitude. The distribution of conics with energies less than 400 eV peaks around local noon. Thus the association between f_{H+} lines and conics, discussed in the next section, is consistent with the statistical properties of conics described by Gorney *et al.* [1981]. Because of the small number of angular windows covered by the Spectro detectors, the nonobservation of conics on AUREOL 3 does not mean that conics are not present. For this reason, it is not easy to carry out a statistical analysis of the associations between waves and suprathermal particles.

5. CORRELATIONS WITH ION DATA

Plate 3 shows data taken along pass 3162. Dynamic spectra of the magnetic components B_x and one electric E_z component are shown in Plates 3a and 3b (in the same format as Plates 2a and 2b). Plate

TABLE 1. Relative Invariant Latitude $\Delta\lambda$ of Equatorward Boundaries of the Lower Invariant Latitude of the LIT and the f_{H+} Observed on the Same Orbit

Day 1982	Orbit	MLT	$\Delta\lambda$
June 15	3517	10	+ 8°
June 8	3425	11	+ 6°
June 8	3426	11	+ 11°
Aug. 23	4429	12	+ 11°
May 17	3136	13	+ 13°
May 19	3162	13	+ 12°
Aug. 16	4337	13	+ 15°
Aug. 17	4350	13	+ 10°
May 12	3071	14	+ 7°
May 12	3069	14	+ 9°
May 4	2965	15	+ 0°
April 28	2887	15	> + 3°
April 8	2624	18	- 1°

3c gives the relative O⁺, H⁺, and He⁺ ion densities, obtained from the Dyction experiment. Plate 3d shows the H⁺ flux measured by the suprathermal ion spectrometers of the Spectro experiment between 10 and 100 eV, in two fixed directions: $\sim 60^\circ$ pitch angle (the curve labeled downgoing ions), and $\sim 120^\circ$ (the curve labeled upgoing ions). As discussed above, we take a higher flux in the upward direction after 1111:00 UT as an indication of the detection of a conical ion distribution. Before 1111:00 UT the ion fluxes are too low to be significant.

Plate 4 shows wave and particle data for one other event, on orbit 3084. This event is similar to the one displayed in Plate 3. After 1321 UT an increase in the flux of the suprathermal H⁺ ions moving up (dashed line in Plate 4e) is observed. It corresponds to a strong depletion in the cold H⁺ and He⁺ ionospheric ions. Simultaneously, the spectrum of the B_x component extends below f_{H+} and a line just below f_{H+} shows up in the E_z component. Moreover, the flux of 10-100 eV ions moving upward is maximum when the f_{H+} line is the most intense. This suggests that the acceleration process of the H⁺ ions is directly related to the appearance of an enhanced line at $f \sim f_{H+}$. Prior to further discussing the relations between these lines at f_{H+} and ion heating, it is necessary to investigate the properties of the wave field close to f_{H+} . This will be done in the next section.

6. WAVE CHARACTERISTICS AROUND F_{H+}

The statistical results presented in the previous section have shown that an enhanced line at f_{H+} is usually observed for ELF emissions where the H⁺ ion concentration is small, which leads us to consider the propagation of waves in a multicomponent plasma with a low H⁺ concentration. Near f_{H+} the percentage of the light ions plays a major role in wave propagation; whenever light H⁺ ions are the minor species, the exact concentration of the various heavy ions is of little importance for frequencies close to f_{H+} . Therefore, to simplify the discussion, we will assume that O⁺ is the only heavy ion.

Dispersion Relation

Figure 5 shows the dispersion relation below f_{H+} in the presence of H⁺ and O⁺ ions. The parameter X is the normalized frequency f/f_{H+} . Clearly, the dispersion relation of ELF waves is greatly modified by the presence of one species of heavy ion. In the absence of heavy ions, the well-known dispersion relation is characterized by two branches: the left-handed ion cyclotron branch, and the right handed magnetosonic branch. In the presence of one additional ion, three new characteristic frequencies (X_{cutoff} , X_{cr} , $X_{\text{bi-ion}}$) appear, and three different branches, referred to as class

ORB 3162 19/05/1982 TROMSOE AUREOL-3

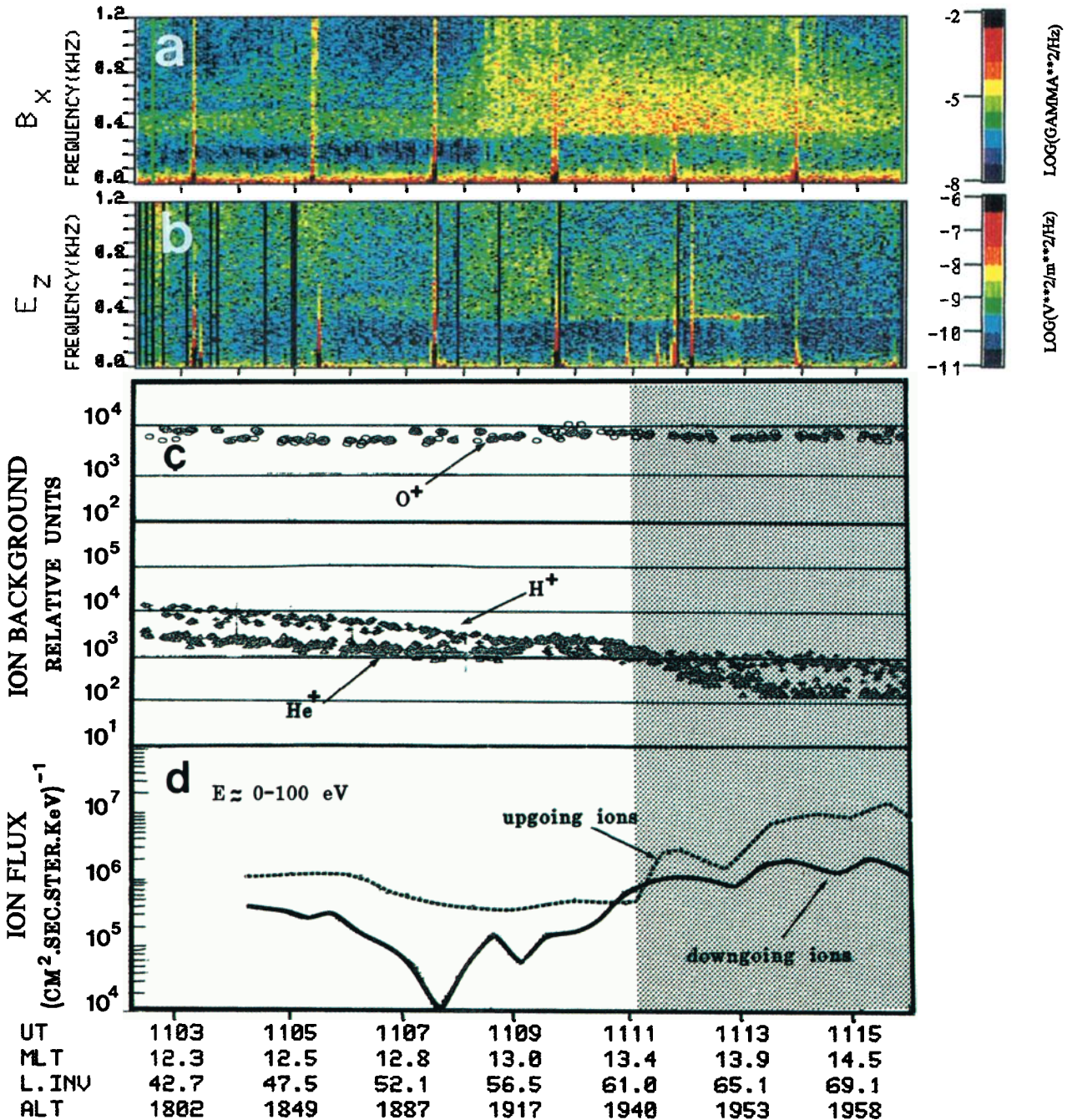


Plate 3. (a) Magnetic (B_x) and (b) electric (E_z) spectrograms taken on May 19, 1982. (c) The relative densities (H⁺, He⁺, H⁺) of the cold plasma. (d) The downgoing and upgoing flux of suprathermal H⁺ ions. From 1111 UT the upgoing flux becomes significant.

I, II, and III, characterize the propagation. Following Rauch et al. [1985], we label as class I the waves which have frequencies below the heavy-ion gyrofrequency (here $X \leq X_{O^+} = 1/16$); they are left-hand polarized with an oblique resonance below X_{O^+} . The dispersion relation of class II waves is more complex; two new characteristic frequencies appear: a new plasma cutoff frequency X_{cutoff} where the wave number $N = Kc/\omega$ becomes zero for any propagation angle, and a new crossover frequency X_c where a polarization reversal occurs. This class has no resonance at the ion gyrofrequency. Class II waves cross the proton gyrofrequency with a purely right-handed polarization. Class III waves propagate below

the proton gyrofrequency ($X \leq X_{H^+} = 1$), and they also reverse their sense of polarization at the crossover frequency. These waves are left handed above X_c and right handed below X_c . In contrast with class II, class III waves have resonances between the bi-ion (X_{bi-ion}) and the proton gyrofrequency ($X = 1$). The bi-ion frequency is a mixed resonance between H⁺ and O⁺ and corresponds to a resonance for perpendicular propagation ($\Theta = \pi/2$). For discussions it is worth keeping in mind that the parallel electric field of class II waves is negligible, but that of class III waves can be quite significant when the polarization becomes linear near an oblique resonance especially if this resonance is close to the proton

ORB 3084 13/05/1982 TROMSOE AUREOL-3

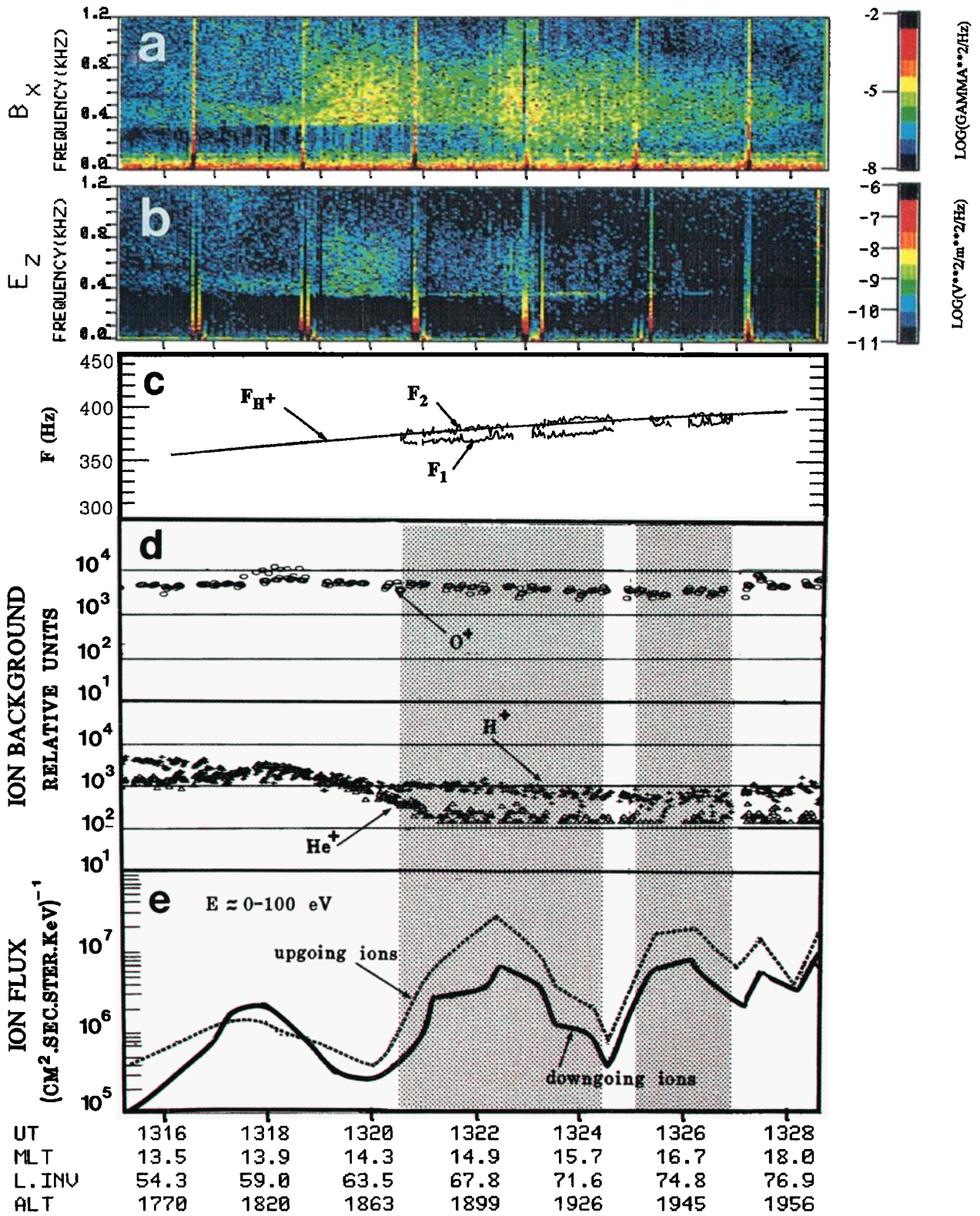


Plate 4. (a) Magnetic (B_x) and (b) electric (E_z) spectrograms taken on May 13, 1982. (c) The minimum frequency F_1 and the maximum frequency F_2 of the peak seen in E_z component. These frequencies are calculated each second. (d) The relative densities (H^+ , He^+ , O^+) of the cold plasma. (e) The downgoing and upgoing flux of suprathermal H^+ ions. From 1321 UT the upgoing flux becomes significant.

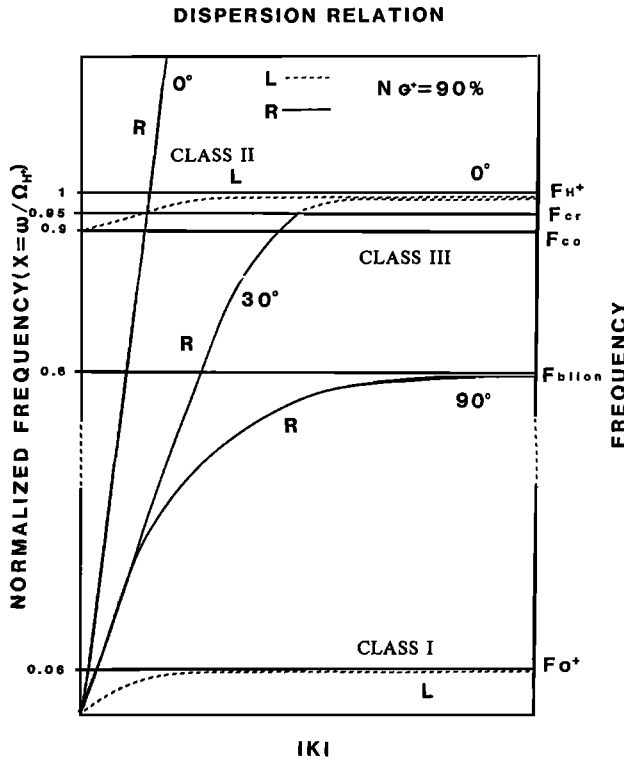


Fig. 5. Dispersion relation of ELF waves in the presence of O⁺ ions (here $N_{O^+}/N_e = 0.90$). The solid curves denote right-hand waves, while the dashed curves denote left-hand waves. Note that the cutoff frequency is very close to the proton gyrofrequency. The dispersions have been drawn for different angles (0°, 30° and 90°) between the wave normal angle K and the static magnetic field B_0 .

gyrofrequency. However, a large E_z can be observed when the mode conversion is operating, because the confluent hypergeometric function describing the electric field diverges rapidly when the wave frequency matches the local proton gyrofrequency, [Le Quéau et al., This issue]

Wave Analysis

The spectra of the five wave components B_x , B_y , B_z , E_H , and E_z have been calculated at two different time intervals selected among the data shown in Plate 3. The three magnetic components have been transformed into a coordinate system linked to the static magnetic field B_0 , so that the z axis is now exactly along B_0 . Figure 6 shows the power spectra at 1110:00 UT, estimated as follows. The waveforms have been Fourier transformed over time intervals of 0.1 s (10-Hz frequency resolution). Power spectra have been estimated from the average of 10 successive Fourier transforms, corresponding to 1 s of signal. The resulting spectra of the magnetic and electric components are represented in Figures 6a and 6b, respectively. The same features are observed in the five components, namely a moderately intense broadband hiss spectrum. A sharp lower-frequency cutoff is seen at the local proton gyrofrequency (363 Hz). Figure 6c shows the angle of propagation θ calculated by Means' method [Means, 1972] from the three magnetic components. As noted by Lefeuvre et al. [1986], however, Means' method does not provide an estimate of θ but an estimate of $\cos(\theta)$. The definition is such that the value of $\cos(\theta)$ is always positive for right-hand polarized waves and negative when for left-hand. Then, the Means angle conveys two different

items of information. First, provided the plane wave hypothesis is valid, i.e., that the Samson [1973] degree of polarization has values close to 1, it gives the angle θ between the wave number K and the magnetic field B_0 (modulo $\pi/2$). Second, even if the field is not that of a plane wave, it gives the sense of polarization of the dominant propagation mode (right for $\theta \leq \pi/2$; left for $\theta \geq \pi/2$). Obviously, both items of information have no physical meaning when the signal-to-noise ratio is too weak.

In Figure 6, the degree of polarization (not shown here) is greater than 0.8 in the region with a significant signal-to-noise ratio (shaded part). In that region the angle θ always takes values of the order of 50°, and the hiss is right-hand polarized. The ellipticity parameter has also been computed from a method suggested by Samson and Olson [1980]. This method, however, is only valid for a plane wave. This is worth remembering when interpreting the results shown in Figure 6d. The polarization is found to be nearly circular, which, together with the right-hand polarization, is consistent in Figure 5 with the type II magnetosonic mode. In any case, this is the only mode that can propagate above the f_{H^+} gyrofrequency in a cold plasma. Several power spectra made in this part of the wave spectrogram show identical features with large θ angles. We interpret the sharp lower-frequency cutoff as a consequence of a large concentration of heavy-ion species [Gurnett et al., 1965] and of a large θ angle [Gurnett and Burns, 1968]. The reason is that for such large values of θ angles the hiss cannot

AUREOL-3

19 5 1982
11 10 0 899 801

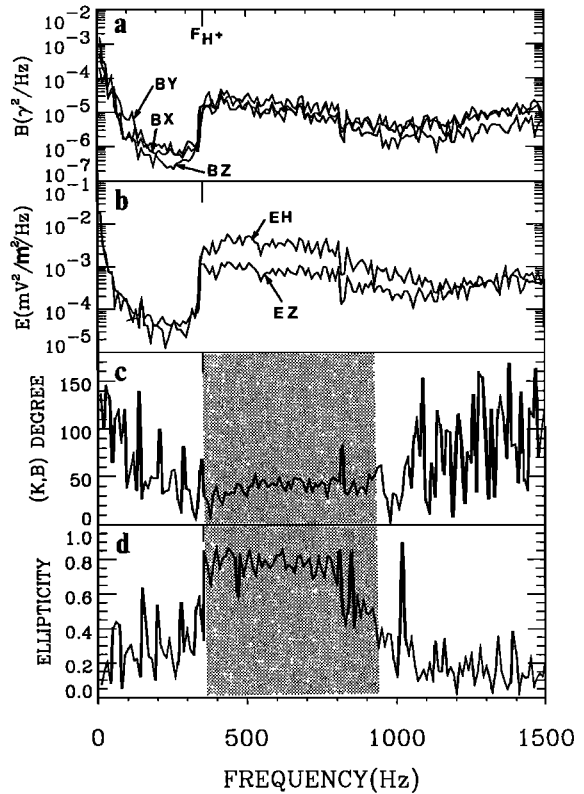


Fig. 6. Spectral characteristics of the five wave field components. (a) and (b) Power spectral densities. The frequency resolution is 10 Hz and the Fourier components have been average over 1 s. (c) Means angle between the wave normal K and the static magnetic field; this parameter is physically meaningful in the frequency band where the power of the waves is strong enough. (d) Ellipticity of the waves, here almost circular.

propagate until the plasma cutoff frequency ($K=0$), because the parallel wave number becomes equal to zero before reaching it. Thus the wave is reflected where its frequency matches the gyrofrequency, or above.

The power spectrum displayed in Figure 7a is different: it corresponds to a time period (1112:20) when the flux of upgoing ions is maximum. The magnetic components have the same spectral shape as in figure 6 with a well-defined lower-frequency cutoff, and the amplitude is the same as in figure 6. The power spectrum of the E_z component, however, is different, as it shows a well-defined peak. The main difference consists in an increase of the power spectrum of E_z just below f_{H^+} . Moreover, the lower-frequency cutoff is slightly below f_{H^+} , and the angle θ is smaller ($\sim 20^\circ$), over a broader frequency range than for the preceding case. Although the estimate of the ellipticity parameter might not be valid over the whole frequency range, Figure 7e suggests that there is a polarization reversal around f_{H^+} . Above f_{H^+} the ellipticity is close to 0.8, which indicates a circularly polarized mode, and just below f_{H^+} it decreases strongly close to 0.2, and the polarization becomes linear. That is consistent with the dispersion relation sketched in Figure 5 if the energy of the wave is propagating from class II to class III. Between f_{H^+} and the cutoff frequency, the waves are essentially propagating a linearly polarized mode. A better frequency resolution will allow us to check this point on the Means θ solutions.

The frequency resolution has been improved as follows. Waveforms have been Fourier transformed over intervals of 10 s each, and these power spectra have been averaged over five successive intervals of 10 s. This is a good compromise to obtain

a good resolution without suffering too much from the change of the f_{H^+} frequency along the trajectory of the satellite. Over 50 s, the proton gyrofrequency has a smaller variation (here 1 Hz) than the width of the peak (here 10 Hz). This high-frequency resolution is used to analyze the spectra of the various electric and magnetic field components shown in Figures 8 and 9. But the level of the spectral power density will be different because we do not use exactly the same analysis period as in Figure 7. It shows a significant decrease in the spectral power density at f_{H^+} and a cutoff significantly below f_{H^+} . The E_z component reaches a large amplitude in a narrow window (~ 7 Hz) right below f_{H^+} . The left-hand polarized line at $f \sim f_{H^+}$ (Figure 8c), since it is always associated with a broadband electromagnetic emission above f_{H^+} (without any discontinuity in the power spectra of the magnetic components around f_{H^+}), is more likely to result from a local mode conversion (from class II to class III) than to result from a local instability (class III). A polarization reversal of the downgoing MSW (class II) at the crossover frequency is a priori possible, but does not account for the existence of a large E_z component. The E_z component is, indeed, negligible for a class II wave, be it right-hand above f_{cr} or left-hand at $f_{\infty} \leq f \leq f_{cr}$. The only branch that is consistent with such a large parallel electric field is the class III, ion cyclotron branch at $f \sim f_{H^+}$ (see Figure 5). Part of the energy of the downgoing class II MSW must have been transferred into a class III proton cyclotron mode; in other words a mode conversion must have taken place. As noticed by *Ngan and Swanson* [1977],

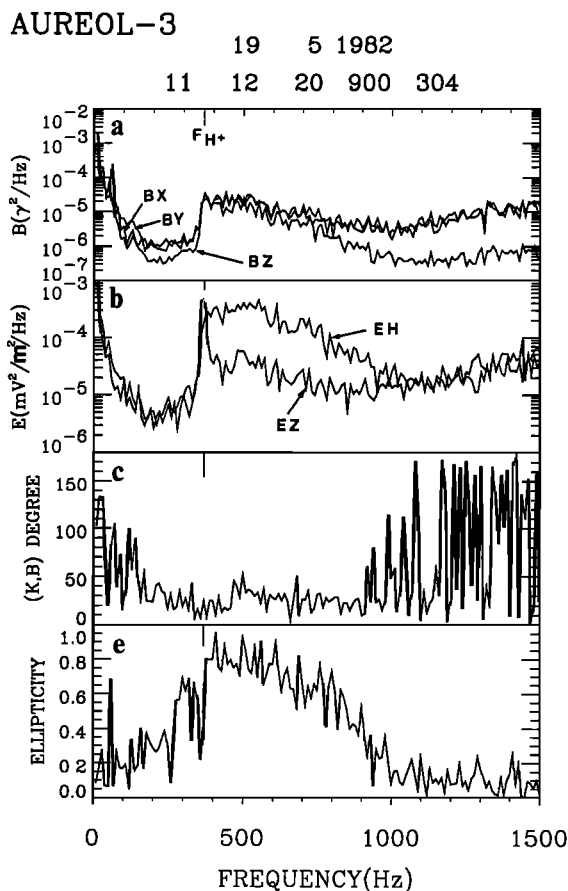


Fig. 7. Same format as Figure 6; note the peak in the E_z component in the vicinity of the proton gyrofrequency.

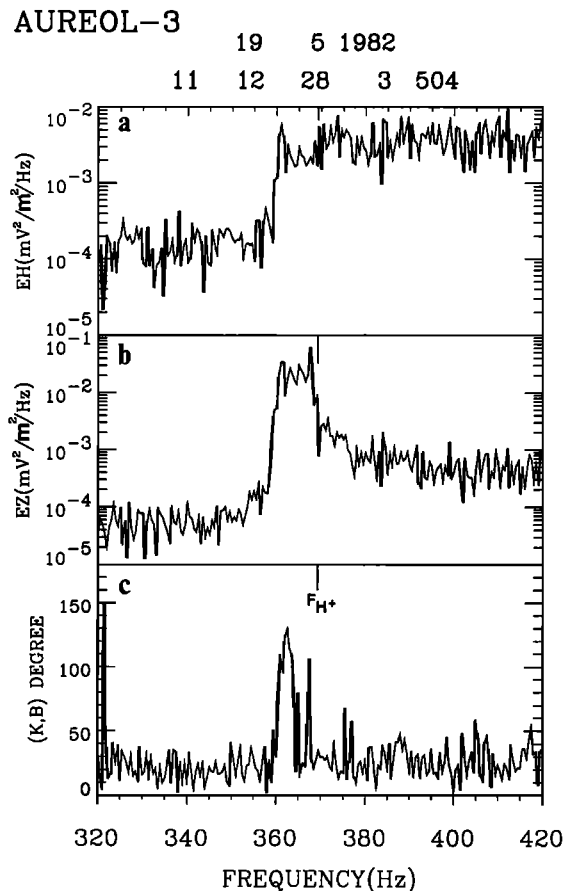


Fig. 8. Power spectral densities of the (a) perpendicular E_H and (b) parallel E_z electric components with a high frequency resolution (here 0.5 Hz) around the proton gyrofrequency. (c) Values of the Means angle (K,B); note the high value greater than 90° at 360 Hz, which indicates a left-hand polarization.

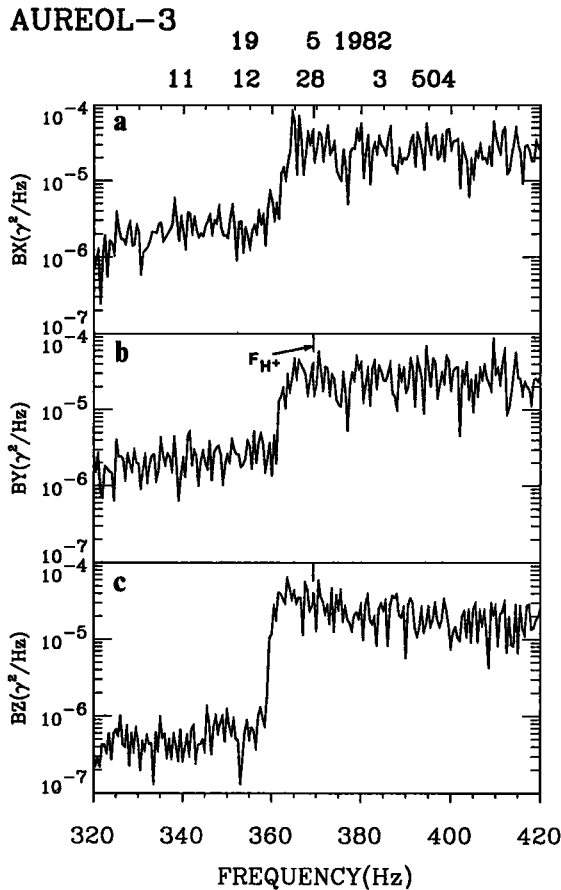


Fig. 9. Power spectral densities of the magnetic components B_x , B_y and B_z . As in Figure 8, the Fourier transform has been made with a resolution of 0.5 Hz. Note the sharp cutoff below the proton gyrofrequency.

the efficiency of the mode conversion strongly depends on the angle of incidence, and only a fraction of the incident energy can be mode converted. This mode conversion process obviously depends on the inhomogeneity of the medium. *White et al.* [1982] have studied the mode conversion of an incident MSW on a deuterium-hydrogen pellet, in the context of laser fusion. These authors have shown that in a range of incident angles a large fraction of the incident MSWs are resonantly absorbed by the protons. *Le Quéau et al.* [this issue] have made a detailed study of the resonant absorption, in a multicomponent inhomogeneous plasma. They estimate the reflection, transmission and absorption coefficients through the resonant layer (the region where $f \sim f_{H+}$). When $N_{O+} \gg N_{H+}$, *Le Quéau et al.* [this issue] find that a large fraction (~25%) of the incident energy can be absorbed in the resonant layer. The absorption rate depends on the ratio N_{H+}/N_{O+} , on the inhomogeneity, and on the angle θ . At AUREOL-3 altitude for $N_{H+}/N_{O+} = 0.01$ the absorption coefficient is $\geq 12\%$, for $30^\circ < \theta < 60^\circ$.

7. SUMMARY AND DISCUSSION

ELF waves observed along the orbit of AUREOL 3 (below 2000 km) are usually consistent with local reflection close to the proton gyrofrequency f_{H+} . When they are observed in the light ion trough (LIT), however, the ELF waves often exhibit a well-defined peak especially in the E_z component, and right below the local f_{H+} . The percentage of occurrence of these lines is very large in the 0900 to

2100 MLT sector. It has been shown that this finite E_z component testifies to the occurrence of a resonant absorption of the incident energy. According to this interpretation, which is discussed by *Le Quéau et al.* [this issue], the enhancement at f_{H+} of the power spectral density in the E_z component is nothing like that of the signature of a mode conversion process. Such a process, which allows an energy transfer to the slow proton cyclotron mode, can lead to the heating of minor H⁺ ions through a resonant absorption mechanism. The full process can therefore account for the transverse acceleration of H⁺, which leads to the formation of conics. As a matter of fact, the distribution of conics has been shown to be consistent with that of the LIT, where resonant absorption has been shown to occur. More direct evidence comes from the correlation between the observed enhancement of the ELF noise with an intense line at $f \sim f_{H+}$, observed together with an increase in the flux of suprathermal H⁺ ions having a higher flux upward than downward.

In Figure 10 the general process is summarized. Precipitating electrons generate the hiss at high altitude. As the hiss propagates downward, waves with a large θ angle are reflected upward, before reaching the gyrofrequency layer. Conversely for small and moderate values of θ , the hiss can reach the regions where $f \leq f_{H+}$. When the wave frequency becomes about the local gyrofrequency f_{H+} , part of the energy undergoes a resonant absorption in a thin layer right below the point where $f \sim f_{H+}$. The absorbed energy is used to accelerate H⁺ ions in the transverse direction. Since the downgoing ELF waves have a broad spectrum, the resonant absorption/heating process can be cumulative. As pointed out by

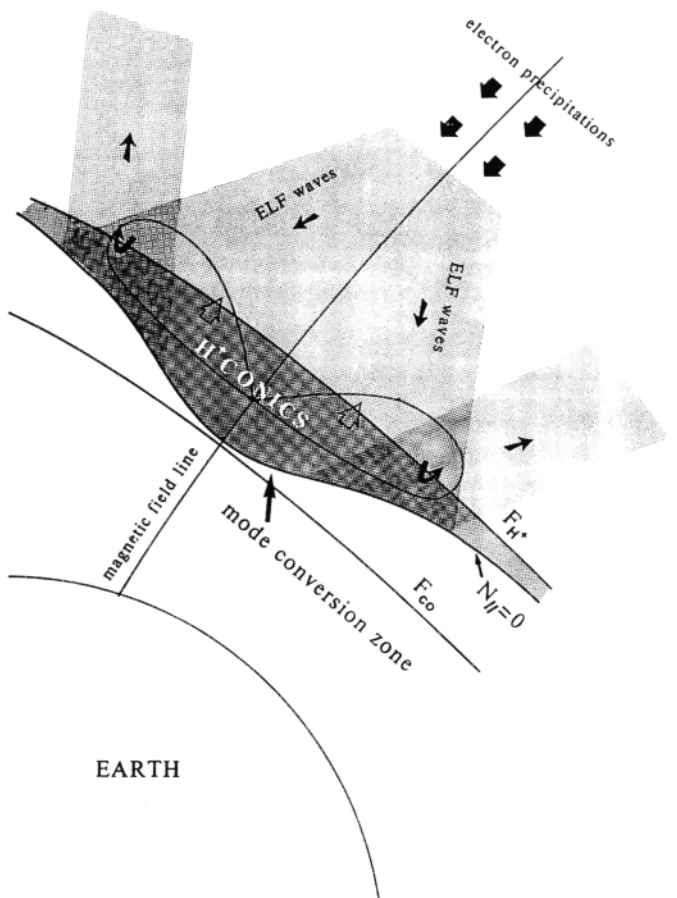


Fig. 10. Sketch which summarizes the formation of H⁺ conics at low altitude.

Crew *et al.* [1990], the H⁺ (or O⁺) heating at various altitudes can add up and therefore lead to a large increase of the energy of ions. The good correlation between the enhanced lines at $f \sim f_{H^+}$ and the LIT strongly suggests that the resonant absorption at $f \sim f_{H^+}$ and the subsequent H⁺ heating only occurs where H⁺ is the minor species, as discussed by Le Quéau *et al.* [this issue]. One can expect the same process to heat O⁺ ions whenever they become the minor constituent of the plasma and when a high level of Alfvén waves exists at $f \sim f_{O^+}$. Such a situation was seldom seen on AUREOL 3, but should occur at higher altitudes.

Acknowledgments. The authors are grateful to the referees for critical reviews of this paper.

The Editor thanks the referees for their assistance in evaluating this paper.

REFERENCES

- André, M., G. B. Crew, W. K. Peterson, A. M. Persoon, C. J. Pollock, and M. J. Engebretson, Ion heating by broadband low-frequency waves in the cusp/cleft, *J. Geophys. Res.*, **95**, 20,809, 1990.
- Ashour-Abdalla, M., and H. Okuda, Turbulent heating of heavy ions on auroral field lines, *J. Geophys. Res.*, **89**, 2235, 1984.
- Berthelier, J. J., J. Covinhes, M. Godefroy, G. Gogly, C. Guerin, D. Roux, P. Thevenet, and V. A. Gladyshev, The thermal ion mass spectrometer on board AUREOL-3: The DYCTION experiment, *Ann. Geophys.*, **38**, 591, 1982a.
- Berthelier, J. J., F. Lefeuvre, M. M. Mogilevsky, O. A. Molchanov, Yu. I. Galperin, J. F. Karczewski, R. Ney, G. Gogly, C. Guerin, M. Leveque, J. M. Moreau, and F. X. Sene, Measurements of the VLF electric and magnetic components of waves and DC electric field on board the AUREOL-3 satellite: The TBF ONCH experiment, *Ann. Geophys.*, **38**, 643, 1982b.
- Bosqued, J. M., H. Barthe, J. Coutelier, J. Crasnier, J. Cuvilo, J. L. Medale, H. Reme, J. A. Sauvaud, and R. A. Kovrazhkin, The low energy electron and ion spectrometers, on the AUREOL-3 satellite: The SPECTRO experiment, *Ann. Geophys.*, **38**, 567, 1982.
- Chang, T., and B. Coppi, Lower hybrid acceleration and ion evolution in the supraauroral region, *Geophys. Res. Lett.*, **8**, 1253, 1981.
- Chang, T., G. B. Crew, N. Hershkowitz, J. R. Jasperse, J. M. Retterer, and J. D. Winningham, Transverse acceleration of oxygen ions by electromagnetic ion cyclotron resonance with broad band left-hand polarized waves, *Geophys. Res. Lett.*, **13**, 636, 1986.
- Crew, G. B., T. Chang, J. M. Retterer, W. K. Peterson, D. A. Gurnett, and R. L. Huff, Ion cyclotron resonance heated conics: Theory and observations, *J. Geophys. Res.*, **95**, 3959, 1990.
- Gorney, D. J., A. Clarke, D. Croley, J. F. Fennell, J. Luhmann, and P. F. Mizera, The distribution of ion beams and conics below 8000 km, *J. Geophys. Res.*, **86**, 83, 1981.
- Gorney, D. J., S. R. Church, and P. F. Mizera, On ion harmonic structures in auroral zone waves: The effect of ion conic damping of auroral hiss, *J. Geophys. Res.*, **87**, 10,479, 1982.
- Guegan, S., G. J. Bailey, R. F. Moffett, R. A. Heelis, T. J. Fuller-Rowell, D. Rees, and R. W. Spiro, A theoretical study of the distribution of ionization in the high-latitude ionosphere and plasmasphere: First results on the mid-latitude trough and the light-ion trough, *J. Atmos. Terr. Phys.*, **44**, 619, 1982.
- Gurnett, D. A., and T. B. Burns, The low frequency cutoff of ELF emissions, *J. Geophys. Res.*, **73**, 7437, 1968.
- Gurnett, D. A., and L. A. Frank, VLF hiss and related plasma observations in the polar magnetosphere, *J. Geophys. Res.*, **77**, 172, 1972.
- Gurnett, D. A., S. D. Shawhan, N. M. Brice, and R. L. Smith, Ion cyclotron whistlers, *J. Geophys. Res.*, **70**, 1665, 1965.
- Horwitz, J. L., R. H. Comfort, P. G. Richards, M. O. Chandler, C. R. Chappell, P. Anderson, W. B. Hanson, and L. H. Brace, Plasmasphere-ionosphere coupling, 2, Ion composition measurements at plasmaspheric and ionospheric altitudes and comparison with modeling results, *J. Geophys. Res.*, **95**, 7949, 1990.
- Johnson, J. R., T. Chang, G. B. Crew, and M. André, Equatorially generated ULF waves as a source for the turbulence associated with ion conics, *Geophys. Res. Lett.*, **16**, 1469, 1989.
- Kintner, P. M., and D. J. Gorney, A search for plasma processes associated with perpendicular ion heating, *J. Geophys. Res.*, **89**, 937, 1984.
- Klumpar, D. M., Transversely accelerated ions: An ionospheric source of hot magnetospheric ions, *J. Geophys. Res.*, **84**, 4229, 1979.
- Klumpar, D. M., A digest and comprehensive bibliography on transverse auroral ion acceleration, in *Ion Acceleration in the Magnetosphere and Ionosphere*, *Geophys. Monogr. Ser.*, vol. 38, edited by T. Chang, p. 389, AGU, Washington, D.C., 1986.
- Laaspere, T., and R. A. Hoffman, New results on the correlation between low energy electrons and auroral hiss, *J. Geophys. Res.*, **81**, 524, 1976.
- Lefeuvre, F., Y. Marouan, M. Parrot, and J. L. Rauch, Rapid determination of the sense of polarization and propagation for random electromagnetic wave fields: Application to GEOS-1 and AUREOL-3 data, *Ann. Geophys.*, **4**, 457, 1986.
- Lennartsson, W., Ion acceleration mechanism in the auroral regions, general principles, in *Energetic Ion Composition in the Earth's Magnetosphere*, edited by R. G. Johnson, p. 43, Terra Scientific, Tokyo, 1983.
- Le Quéau, D., A. Roux, J. L. Rauch, F. Lefeuvre, and J. M. Bosqued, Heating of protons by resonant absorption in a multicomponent plasma, 2, Theoretical model, *J. Geophys. Res.*, this issue.
- Lundin, R., G. Gustafsson, A.I. Eriksson, and G. Marklund, On the importance of high-altitude low-frequency electric fluctuations for the escape of ionospheric ions, *J. Geophys. Res.*, **95**, 5905, 1990.
- Lysak, R., M. K. Hudson, and M. Temerin, Ion heating by strong electrostatic ion cyclotron turbulence, *J. Geophys. Res.*, **85**, 678, 1980.
- Means, J. D., The use of the three dimensional covariance matrix in analyzing the properties of plane waves, *J. Geophys. Res.*, **77**, 5551, 1972.
- Moser, F. S., Analyses of techniques for measuring DC and AC electric fields in the magnetosphere, *Space Sci. Rev.*, **14**, 272, 1973.
- Mosier, S. R., and D. A. Gurnett, Observed correlations between auroral and VLF emissions, *J. Geophys. Res.*, **77**, 1137, 1972.
- Ngan, Y. C., and D. G. Swanson, Mode conversion and tunneling in an inhomogeneous plasma, *Phys. Fluids*, **20**, 1920, 1977.
- Okuda, H., and M. Ashour Abdalla, Formation of a conical distribution and intense ion heating in the presence of hydrogen cyclotron waves, *Geophys. Res. Lett.*, **8**, 811, 1981.
- Okuda, H. and M. Ashour-Abdalla, Acceleration of hydrogen ions and conics formation along auroral field lines, *J. Geophys. Res.*, **88**, 899, 1983.
- Parrot, M., World map of ELF/VLF emissions as observed by a low-orbiting satellite, *Ann. Geophys.*, **8**, 135, 1990.
- Rauch, J. L., and A. Roux, Ray tracing of ULF waves in a multicomponent magnetospheric plasma: Consequences for the generation mechanism of ion cyclotron waves, *J. Geophys. Res.*, **87**, 8191, 1982.
- Rauch, J. L., F. Lefeuvre, J. C. Cerisier, J.J. Berthelier, N. Boudko, G. Michailova, and O. Kaspustina, Attenuation bands and cut off frequencies for ELF electromagnetic waves, in *CNES-Results of the ARCAD-3 PROJECT and of the Recent Programmes in Magnetospheric Physics*, p. 435, Cepadues-Editions, Toulouse, 1985.
- Retterer, J. M., T. Chang, and J. R. Jasperse, Ion acceleration by lower hybrid waves in the supraauroral region, *J. Geophys. Res.*, **91**, 1609, 1986.
- Samson, J. C., Description of the polarisation state of vector processes: application to ULF magnetic fields, *Geophys. J. R. Astron. Soc.*, **34**, 403, 1973.
- Samson, J. C., and J. V. Olson, Some comments on the descriptions of the polarization states of waves, *Geophys. J. R. Astron. Soc.*, **61**, 115, 1980.
- Sharp, R. D., A. G. Ghielmetti, R. G. Johnson, and E. G. Shelley, Hot plasma composition results from the S3-3 spacecraft, in *Energetic Ion Composition in the Earth's Magnetosphere*, editing by R. G. Johnson, p. 23, Terra Scientific, Tokyo, 1983.
- Taylor, H. A., Jr. and W. J. Walsh, The light-ion trough, the main trough, and the plasmopause, *J. Geophys. Res.*, **77**, 6716, 1972.
- Ungstrup, E., D. M. Klumpar, and W. J. Heikkila, Heating of ions to superthermal energies in the topside ionosphere by electrostatic ion cyclotron waves, *J. Geophys. Res.*, **84**, 4289, 1979.
- White, R. B., S. Yoshikawa, and C. Oberman, Alfvén wave cyclotron resonance heating, *Phys. Fluids*, **25**, 384, 1982.
- Yau, A. W., B. A. Whalen, W. K. Peterson, and E. G. Shelley, Distribution of upflowing ionospheric ions in the high-altitude polar cap and auroral ionosphere, *J. Geophys. Res.*, **89**, 5507, 1984.
- Yau, A. W., P. H. Beckwith, W. K. Peterson, and E. G. Shelley, Long-term (solar cycle) and seasonal variations of upflowing ionospheric ion events at DE 1 altitudes, *J. Geophys. Res.*, **90**, 6395, 1985a.
- Yau, A. W., E. G. Shelley, W. K. Peterson, and L. Lenchyshyn, Energetic auroral and polar ion outflow at DE 1 altitudes: Magnitude, composition, magnetic activity dependence, and long-term variations, *J. Geophys. Res.*, **90**, 8417, 1985b.

J. J. Berthelier, Centre de Recherche en Physique de l'Environnement, Centre National d'Etude des Télécommunications, Centre National de la Recherche Scientifique, 4 Avenue de Neptune, 94107 Saint Maur des Fossés Cedex, France.

J. M. Bosqued, Centre d'Etude Spatial des Rayonnements, Centre National de la Recherche Scientifique, 9 Avenue du Colonel Roche, F-31029 Toulouse Cedex, France.

F. Lefeuvre and J. L. Rauch, Laboratoire de Physique et Chimie de l'Environnement, Centre National de la Recherche Scientifique, 3A Avenue de la Recherche Scientifique, F-45071 Orléans Cedex 2, France.

D. Le Quéau, Entité Centre de la Recherche Scientifique du Centre

de Recherche en Physique de l'Environnement - 10, 12, Avenue de l'Europe, 78140 Vélizy, France.

A. Roux, Centre de Recherche en Physique de l'Environnement, Centre National d'Etude des Télécommunications, Centre National de la Recherche Scientifique, 38-40 rue du Général Leclerc, 92131 Issy-les-Moulineaux Cedex, France.

(Received November 5, 1990;
revised June 9, 1992;
accepted September 9, 1992.)